Fundamental properties of high-order harmonic generation from field-free aligned molecules with intense femtosecond laser pulses

Kenzo Miyazaki, Godai Miyaji, Masanori Kaku, and Kazumichi Yoshii

Advanced Laser Science Research Section, Institute of Advanced Energy, Kyoto University, Gokasho, Uji, Kyoto 611-0011, Japan

This paper reports fundamental aspects of high-order harmonic generation from N_2, O_2 and CO_2 molecules spatially aligned with intense femtosecond laser pulses. The time-dependent harmonic signal observed with a pump and probe technique has been found to include several sets of beat frequency for pairs of coherently populated rotational states. We have shown the origin of each frequency component and its effect on the revival signal. The results demonstrate that the high-order harmonic generation provides a sensitive and useful way for an extensive study of dynamic processes in the field-free alignment of molecules.

OCIS codes: 190.4160, 190.7110, 020.1670, 270.4180.

Intense ultrashort laser pulses are able to non-adiabatically induce alignment of molecules that is recurrent under field-free conditions[1,2]. There has been much interest in this field-free alignment of molecules, since it provides a promising approach to control molecules with an external field for a variety of applications[3]. Recently it has been demonstrated that the dynamic alignment of molecules can be detected with high-order harmonic generation (HHG) by intense femtosecond laser pulses[4,5]. The characteristic HHG observed demonstrates an effective approach to extensively study wave packet dynamics and also suggests a possible new area of nonlinear optics which uses the molecular wave packet to control the strong-field interaction. This paper reports the fundamental aspect of the HHG from field-free aligned molecules in time and frequency domains, where we focus our attention on the temporal evolution of harmonic yield from the wave packet in N_2, O_2 and CO_2 molecules and their frequency spectra.

We consider a pump-probe experiment using nonresonant, linearly polarized ultrashort laser pulses for a simple linear molecule. The pump pulse forms a rotational wave packet,

$$\Psi_g(t) = \sum_J a_J \psi_{JM} \exp(-iE_J t/\hbar), \qquad (1)$$

where ψ_{JM} is the field-free rotor wave function, pertaining to the eigenenergy $E_J = 2\pi\hbar BcJ(J+1)$, c is the light speed in vacuum, for the rotational state with the angular momentum J and its projection M on the field direction, and the coefficient a_J is almost independent on time after interaction[1,2]. Equation (1) brings about molecular alignment and its field-free revivals at a period of $T_{\rm rev} = 1/(2Bc)$ with the rotational constant B. It is well known that the degree of alignment is characterized by the expectation value $\langle\cos^2\theta\rangle$ calculated with $\Psi_g(t)$, where θ is the angle between the molecular axis and the field direction. The time-dependent behavior of $\langle\cos^2\theta\rangle$ is dominated by beats at frequency $\omega_1 = 2\pi Bc(4J+6)$ between any pair of rotational states J and $J\pm2$ that are populated through the transition, $\Delta J \equiv J - J' = 0, \pm2$ with $\Delta M = 0$. The delayed probe pulse generates high harmonic radiation from the wave packet. The HHG from a single molecule is essentially a single-cycle event in the laser field[6], while the temporal harmonic signal observed as a function of time delay Δt between pump and probe pulses is very slow and would predominantly be governed by the beat at ω_1 as for $\langle\cos^2\theta\rangle$.

In the experiment, we used a Ti:sapphire laser to produce pulse energy of 40 mJ in 40-fs pulses at 800 nm. The linearly polarized output was split into two beams to produce a variable time delay Δt between pump and probe pulses. The two beams were recombined collinearly and focused with a 50-cm focal-length lens into a pulsed molecular beam jetted from a 1-mm-diameter nozzle. The gas pressure in the jet was typically 10 Torr. The pump pulse intensity was in a range of $(4-8)\times10^{13}$ W/cm^2, and the probe was slightly more intense than the pump. The harmonic radiation was detected by an electron multiplier mounted on a vacuum ultraviolet monochromator, and the signal processed by a boxcar averager was stored on a personal computer. In the preliminary experiment we observed the time-dependent signal for all orders of harmonic higher than the 15th for which the semi-classical model[6] would be valid. Since their revival structures represented no fundamental difference, we selected the 19th harmonic ($\lambda \sim 42.1$ nm) for the present study.

Figure 1 shows a typical example of the harmonic signal observed for N_2 as a function of Δt and its frequency spectrum. We have confirmed that the observed signal shown in Fig. 1(a) is well reproduced by the simulated result of $\langle\cos^2\theta\rangle$, except for the signal at $\Delta t \sim 0$[5]. This indicates that the 19th harmonic is most efficiently produced with N_2 molecules aligned parallel to the probe pulse field and suppressed with those aligned perpendicularly, as reported so far[4,5]. The detailed revival structure has been discussed by comparing the observed signal with the simulated $\langle\cos^2\theta\rangle$[5]. Briefly, the initial signal drop at $\Delta t \sim 0$ is due to strong ionization induced by the intense superimposed pump and probe pulses. The onset of alignment is shown by the first peak at $\Delta t \sim 0.2$ ps after the pump pulse interaction, as suggested by our previous study[7]. This signal peak rapidly

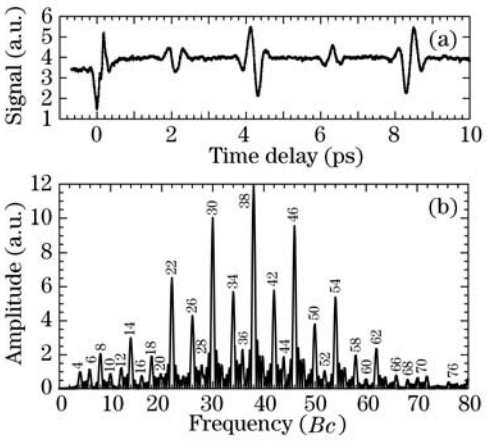

Fig. 1. (a) 19th harmonic signal observed for N_2 as a function of time delay between the pump and probe pulses at the intensities of 0.8×10^{14} and 1.7×10^{14} W/cm^2, respectively, and (b) its frequency spectrum in which the number on each spectral peak denotes the frequency at ω_1, ω_2 and ω_3 in Bc.

decreases due to dephasing of rotational states in the wave packet. The full revival of alignment is observed at $\Delta t \sim 8.5$ ps, corresponding to $T_{\rm rev} = 8.3$ ps with $B = 2$ cm^{-1} for N_2, where the rapid signal modulation is due to the rotation of aligned molecules.

The frequency spectrum shown in Fig. 1(b) represents the structure of the rotational wave packet. The spectrum is mainly composed of strong beat frequencies (6, 10, 14, 18, $\cdots$) at ω_1 with a separation $\Delta\omega_1/2\pi = 4Bc$, as expected from $\langle\cos^2\theta\rangle$. The spectral amplitude in this *allowed series* is larger for the even J and weaker for the odd J. This intensity alternation originates from the population ratio 2:1 between the even- and odd-J states of N_2[8].

The spectrum shown in Fig. 1(b) includes an additional set of frequency component (20, 28, 36, 44, $\cdots$) at $\omega_2 = (E_{J+4} - E_J)/\hbar = 2\pi Bc(8J + 20)$ with a separation of $8Bc$ for a pair of rotational states J and $J \pm 4$. As discussed in our recent paper[5], this *Raman-forbidden series* arises from the expectation value of $\langle\cos^4\theta\rangle$, and the coherence between the rotational states for $\Delta J = \pm 4$ would be created by multi-step Raman transitions during the wave packet formation process. Then, the spectral amplitude at ω_2 should be much weaker than that at ω_1. We notice that the signal amplitude at ω_2 is peaked for $J = 1 - 3$. This suggests that the high population of low J states at the initial low temperature in the gas jet is responsible for the high-order coherence to be detected with the HHG. The weaker frequency component at ω_2 has also been observed in the high-frequency region for $J = 8 - 13$ due most likely to the redistribution of rotational states through the pump process[5]. The time-dependent signal from the ω_2 component is easily shown to have the revival period of $T_{\rm rev}/2 = 1(4Bc)$, as discussed later.

In Fig. 1(b), we see the third set of weak component (4, 8, 12, 16, $\cdots$) at ω_3. As shown by the recent theory developed[9], this *anomalous series* is originated from the expectation value of the form $\langle\cos^2\theta\rangle\langle\cos^2\theta\rangle$ that leads to $\omega_3 = 2\pi Bc[4(J + J') + 12]$, and $2\pi Bc[4(J - J')]$. In contrast to the ω_1 series, this anomalous series appears to be produced with only adjacent low J states. This suggests that, as for the Raman-forbidden series at ω_2, the high-order coherence is efficiently created with the initial high population of low J states. We note that the HHG reveals such high-order coherence embedded in the rotational wave packet, demonstrating the high sensitivity for detecting the *rotational coherence* created by the pump pulse.

As shown in Fig. 1(b), the time-dependent harmonic signal is predominantly governed by the frequency component at ω_1. To see the contribution of the even- and odd-J components to the revival structure, we reconstructed the temporal evolution of the harmonic signal with the inverse Fourier transform for each component, and the result is shown in Fig. 2. It is clearly shown that the even- and odd-J components contribute in anti-phase to the revival signals at $T_{\rm rev}/4$ and $3T_{\rm rev}/4$ to produce the small peak due to the population difference, while the signal in phase at $T_{\rm rev}/2$ and $T_{\rm rev}$ creates a large modulation in the harmonic signal.

Figure 3 shows the time-dependent 19th harmonic signal for O_2 and its frequency spectrum. In Fig. 3(a), the full revival is seen at $T_{\rm rev} \sim 11.6$ ps, corresponding to $B = 1.44$ cm^{-1} for O_2. The revival signals at multiples of $T_{\rm rev}/4$ represent almost the same amplitude, since only odd-J states are populated in the ground state of O_2 having no nuclear spin. The observed harmonic yield as well as the revival signal was much smaller than that for N_2. The low HHG efficiency would result from the anti-symmetric structure of molecular orbital. We tried to find a different angle α between the pump and probe field directions to produce a larger revival signal, but the best signal modulation was observed at $\alpha \sim 0°$, as well as the highest harmonic yield. This is inconsistent with the previous conclusion[10] that the HHG from aligned O_2 is peaked at $\theta \sim 45°$ and minimized at $\theta \sim 0°$ and 90°, although θ is different from α. Recently, the α-dependent HHG observed has been shown to reconcile with the theoretical result.

The frequency spectrum shown in Fig. 3(b) consists

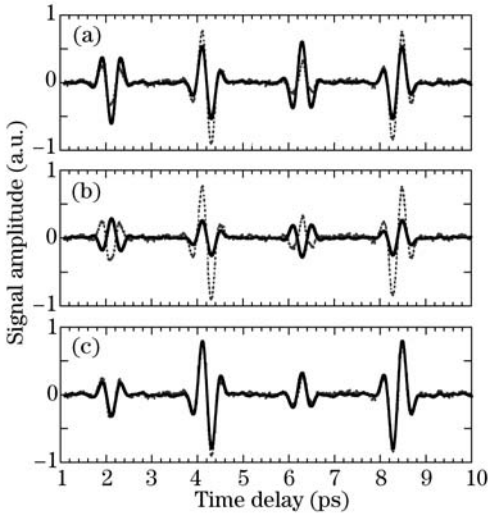

Fig. 2. Time-dependent 19th harmonic signals (solid lines) reproduced with the inverse Fourier transform for (a) the even-J component, (b) odd J, and (c) both of even and odd J. For comparison, each trace includes the observed signal (gray dashed lines).

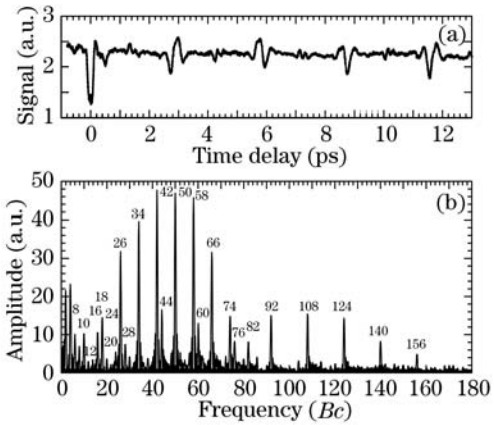

Fig. 3. (a) 19th harmonic signal observed for O_2 as a function of time delay at the pump and probe intensities of 0.5×10^{14} and 1.2×10^{14} W/cm^2, respectively, and (b) its frequency spectrum in which the number on each spectral peak denotes the frequency at ω_1, ω_2 and ω_3 in Bc.

of the strong component at ω_1 and the weak at ω_2 and ω_3 for odd J. We note that the spectral peaks at ω_1 (42−58) correspond to those at ω_2 (92−124) for almost the same values of $J = 9 - 13$. This confirms that the ω_2 component certainly originates from the beat between the rotational states J and $J \pm 4$ that are coherently populated in the wave packet. The spectrum shown in Fig. 3(b) involves a set of ω_2 (28−76) with a sub-peak for $J = 3$. As discussed above, the ω_2 component in the low frequency region accounts for the initial low temperature $T_{\rm rot}$ in the supersonic gas jet. Our simulation has shown that the spectral peak for $J = 3$ corresponds to $T_{\rm rot} = 25 - 50$ K.

In Fig. 3(b), the ω_3 component (8, 12, 16, 20, $\cdots$) is also seen in the low frequency regions, as in the N_2 spectrum. The theory has shown that the time-dependent 19th harmonic signal for O_2 are dominated with the expectation values arising from $\langle \cos^2\theta \sin^2\theta \rangle^2$[9]. This term includes the frequencies ω_1, ω_2 and ω_3 coming from $\langle \cos^2\theta \rangle$, $\langle \cos^4\theta \rangle$ and $\langle \cos^2\theta \rangle \langle \cos^2\theta \rangle$, respectively. Since the temporal evolution of $\langle \cos^2\theta \rangle$ includes neither ω_2 and ω_3 components, the coherence at ω_2 and ω_3 embedded in the wave packet is certainly detected through the anisotropic electronic response to the linearly polarized probe pulse used for the HHG.

We tried to reconstruct the time-dependent harmonic signal with the inverse Fourier transform, using two components at ω_1 and ω_2, since the ω_3 component was very weak. The result presented in Fig. 4 demonstrates that the ω_1 component certainly creates the revival signals at $mT_{\rm rev}/4$ with the positive integer m, and the ω_2 component produces the small revival signals at $mT_{\rm rev}/8$ with the full revival period of $T_{\rm rev}/2$. Thus the revival signals at $(2m-1)T_{\rm rev}/8$ in Fig. 3(a) predominantly arise from the ω_2 component. The time-dependent harmonic signal observed is the simple superposition of those arising from the components at ω_1 and ω_2.

The weak 1/8-revival signals for O_2 was also observed so far with the Coulomb explosion imaging[11], where $\langle \cos^2 m\theta \rangle$ was used to analyze the fractional revivals. No observation of the ω_3 component was reported so far. On the other hand, the analysis with $\langle \sin^2 2\theta \rangle$ was

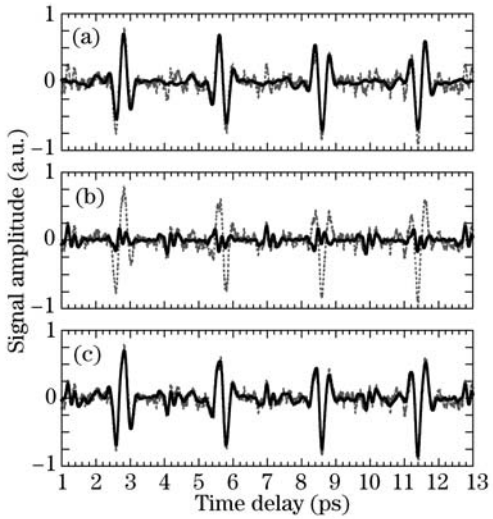

Fig. 4. Time-dependent 19th harmonic signals (solid lines) reproduced for the frequency component at (a) ω_1, (b) ω_2, and (c) ω_1 and ω_2. For comparison, each trace includes the observed signal (gray dashed lines).

empirically introduced to reproduce the time-dependent harmonic signal for O_2[10]. The recent theory has successfully elucidated the origin of the frequency components observed[9].

We have also observed the time-dependent 19th harmonic signal for CO_2. The initial alignment was induced at $\Delta t \sim 0.2$ ps after the pump pulse interaction was over, while the harmonic signal was completely reversed to those of N_2 and O_2. This result suggests that the 19th harmonic is minimized with CO_2 aligned along the pump pulse polarization and peaked with those aligned perpendicularly. The theoretical analysis has shown that this is due to the characteristic electronic response of the highest occupied molecular orbital of the ground state of CO_2 at the 19th harmonic energy, rather than the destructive interference of recombining electron wave proposed so far[12,13]. The experimental results on the harmonic signal phase will be presented and discussed in a separate paper.

In summary, we have demonstrated the fundamental aspects of HHG from rotational wave packets created by the intense femtosecond laser pulse. The present results should be useful for controlling rotational wave packets with ultrashort laser pulses and nonlinear optical processes in molecules.

K. Miyazaki's e-mail address is miyazaki@iae.kyoto-u.ac.jp.

References

1. L. Cai, J. Marango, and B. Friedrich, Phys. Rev. Lett. **86,** 775 (2001).
2. T. Seideman, J. Chem. Phys. **115,** 5965 (2001).
3. H. Stapelfeldt and T. Seideman, Rev. Mod. Phys. **75,** 543 (2003), and references therein.
4. M. Kaku, K. Masuda, and K. Miyazaki, Jpn. J. Appl. Phys. **43,** L591 (2004).
5. K. Miyazaki, M. Kaku, G. Miyaji, A. Abdurrouf, and F. H. M. Faisal, Phys. Rev. Lett. **95,** 243903 (2005).

6. P. B. Corkum, Phys. Rev. Lett. **71,** 1994 (1993).
7. K. Miyazaki, T. Shimizu, and D. Normand, J. Phys. B: At. Mol. Opt. Phys. **37,** 753 (2004).
8. G. Herzberg, *Molecular Spectra and Molecular Structure, I. Spectra of Diatomic Molecules* (Van Nostrand Reinhold, New York, 1950) Chap.III.
9. F. H. M. Faisal, A. Abdurrouf, K. Miyazaki, and G. Miyaji, Phys. Rev. Lett. **98,** 143001 (2007).
10. J. Itatani, D. Zeidler, J. Levesque, M. Spanner, D. M. Villeneuve, and P. B. Corkum, Phys. Rev. Lett. **94,** 123902 (2005).
11. P. W. Dooley, I. V. Litvinyuk, K. F. Lee, D. M. Rayner, M. Spanner, D. M. Villeneuve, and P. B. Corkum, Phys. Rev. A **68,** 023406 (2003).
12. T. Kanai, S. Minemoto, and H. Sakai, Nature **435,** 470 (2005).
13. C. Vozzi, F. Calegari, E. Benedetti, J.-P. Caumes, G. Sansone, S. Stagira, M. Nisoli, R. Torres, E. Heesel, N. Kajumba, J. P. Marangos, C. Altucci, and R. Velotta, Phys. Rev. Lett. **95,** 153902 (2005).